

The Use of Finite Element Methods (FEM) in the Modeling of Localized Corrosion

by C. Liu and R. G. Kelly

Localized corrosion is characterized by intense dissolution at discrete sites on the surface of a metal or alloy, while the remainder of the surface corrodes at a much lower rate. The ratio of the two rates is on the order of 10^9 . Typical forms of localized corrosion include crevice corrosion, pitting, stress corrosion cracking, and intergranular corrosion.¹ Localized corrosion represents the primary corrosion failure mode for passive/corrosion resistant materials.

There has been extensive experimental characterization of the dependence of the susceptibility to corrosion on alloy and solution composition, temperature, and other variables. Computational modeling can play an important role in improving the understanding of localized corrosion processes, in particular when it is coupled with experimental research that accurately quantifies the important characteristics that control corrosion rate and resultant morphology. There are many modeling methods that can be applied, with the choice of method driven by the goal of the modeling exercise.

Empirical models² can be used to predict performance within the parameter space for which they are created. Such models can provide insight into what kinds of processes might be dominating the corrosion process, but further dissection of controlling factors is more difficult.

Numerical modeling, in which the concentration, potential, and current distributions are calculated, plays a role in helping to understand controlling factors. There are several numerical methods that have been implemented by corrosion scientists and engineers. Among these, the finite element method (FEM) has been the most widely used to investigate transport phenomena in systems undergoing.

The finite element method (FEM) is a numerical technique used to obtain approximate solutions to the differential equations that describe a wide variety of physical phenomena, ranging from electrical and mechanical systems to chemical and fluid flow problems. Generally, FEM establishes credible stability criteria and provides more flexibility (e.g., in handling inhomogeneity and complex geometries) compared to other numerical modeling methods such as the finite difference method (FDM). The finite element approach in corrosion study was introduced in the early 1980s by Alkire, Forrest, and Fu.³⁻⁵ The FEM approach has demonstrated an ability to predict electrochemical parameters such as potential and current distributions for localized corrosion.

FEM Modeling in Localized Corrosion

In the general case, the Nernst-Planck Equation, suitable for dilute solutions, is applied as the governing equation in FEM modeling for localized corrosion. The basic form⁶ of this equation can be formulated as

$$\frac{\partial c_i}{\partial t} = \underbrace{\nabla \cdot (D_i \nabla c_i)}_{\text{Diffusion}} + \underbrace{\frac{z_i F}{RT} \nabla \cdot (D_i c_i \nabla \Phi)}_{\text{Migration}} - \underbrace{\nabla \cdot (c_i \mathbf{v})}_{\text{Convection}} + \underbrace{R_i}_{\text{Reaction}} \quad (1)$$

where c_i is the concentration of species i , D_i is the diffusivity of species i , z_i is the charge of species i , F is Faraday's constant, Φ is the electric potential, \mathbf{v} is the fluid velocity, and R_i is rate of homogeneous production of species i . In general the convection term is neglected in localized corrosion modeling, although Harb and Alkire⁷ have shown the conditions under which convection at the mouth of a pit

can influence the conditions inside the pit. A common assumption in mathematical modeling of transport phenomena in electrochemical systems is electroneutrality

$$\sum_{i=1}^n z_i c_i = 0 \quad (2)$$

Electroneutrality states that any volume of solution is electrically neutral due to the large restoring force resulting from any separation of charge.

The solution to the Nernst-Planck equation results in full transient descriptions of the distributions of chemical composition, potential, and current density. The costs of obtaining this complete data set are computational complexity and time. The wide range of time scales that must be taken into account in modeling localized corrosion include very fast processes (ion reaction and response to potential gradients) and slow processes (diffusion of uncharged species under a concentration gradient). This range of timescales, combined with the mathematical difficulties in dealing with highly nonlinear boundary conditions (electrochemical kinetics) make the calculations very difficult, requiring very small time steps and highly refined spatial meshing.

Recent work⁸⁻¹² has shown the usefulness of the application of the Laplace Equation (Eq. 3) to model steady state current and potential distributions under thin-electrolyte conditions.

$$\nabla^2 \Phi = 0 \quad (3)$$

Rather than solving for the full transient, the use of the Laplace Equation approach relies instead on a knowledge or estimation of the electrolyte characteristics (primarily conductivity) and its dependence on position and other experimental variables. This approach ignores diffusive transport contributions to the current density. It has been shown that reasonable estimations of important characteristics of the thin electrolytes forming under atmospheric conditions can be made based on a limited number of measurements and equilibrium calculations. Accurate measurement of the electrochemical kinetics is far more important in determining the success of the model predictions.

Below, two explicit examples regarding applications of FEM in localized corrosion modeling using the simplification of the Laplace equation are presented. The first example presents the use of FEM modeling to predict intergranular corrosion (IGC) damage caused by galvanic interactions in a thin electrolyte. The second example describes a FEM-based model combined with rigorously controlled crevice geometry for the study of crevice corrosion scaling factors.

FEM Modeling to Predict IGC Damage Caused by Galvanic Interactions¹⁰

In experimental work, Mizuno and Kelly¹³ quantitatively investigated the galvanic interaction between sensitized aluminum alloy AA5083-H131 and AISI 4340 steel for samples exposed to a variety of atmospheric and full immersion conditions. A linear correlation was found between the maximum depth of IGC damage and the electrochemical potential under full immersion conditions. Scanning Kelvin Probe measurements of the potential along a galvanic couple of AA5083-H131 and 4340 steel exposed to a thin electrolyte layer were made to demonstrate that the same potential dependence applied to atmospheric conditions.¹³ However, it is

(continued on next page)

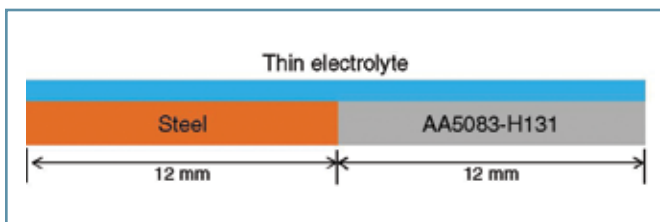


Fig. 1. Geometry in FEM Model representative of a galvanic couple between AA5083-H131 and AISI 4340. Water layer thickness determined by relative humidity (RH) and loading density (LD) of salt according to Chen, et al.¹⁴

difficult to comprehensively measure potential distributions during atmospheric corrosion because many environmental factors affect IGC propagation. Computational modeling can be utilized to simulate potential distribution in the corrosion system, and IGC propagation can be predicted from the simulated potential distributions under atmospheric conditions.

The geometry used is shown in Fig. 1, representing a galvanic couple that occurs when a 4340 steel fastener is coupled with sensitized AA5083-H131. The Nernst-Planck equation was used as the governing equation as implemented in a commercial computational code, and the boundary conditions used were based on electrochemical kinetics parameters fitted to the Butler-Volmer equations from experimentally determined polarization curves.¹³ The calculations were made for $t = 0$, preventing any solution chemistry change or diffusion from occurring. Thus, the governing equation was effectively the Laplace equation. Optimization of the boundary conditions was performed to reproduce the observed galvanic corrosion behavior as a function of degree of sensitization (DoS) and NaCl concentration.

The calculated potential distribution was converted to the IGC depth using the correlation determined from the full immersion testing.¹³ Fig. 2 presents an example of the comparison of the IGC depth distributions between the model calculations and experimental results. Although the experimentally observed IGC depth had significant variability even at the same distance from the steel fastener, the calculations showed IGC distributions very similar to those of the experiments for the entire range of DoS. In addition to reasonably predicting the depth of attack, the modeling predicted with reasonable accuracy the maximum distance from the steel at which IGC damage was observed.

The utility of FEM modeling is shown in Fig. 3, where the calculated maximum IGC depth as a function of RH for these DoS levels is presented. The modeling allows rapid exploration of the effects of the range of important variables. We can gather that the most severe attack is expected to occur at approximately RH = 90% for all DoS levels, that the minimally sensitized specimen (DoS=10 mg/cm²) is not susceptible to IGC when the RH is higher than 95% or lower than 80%, and that the influence of DoS on maximum IGC depth saturates above a DoS of 40 mg/cm². Such FEM-based models can be used to guide experiments and to provide inputs for predicting lifetime and maintenance requirements for structures of interest.

FEM Modeling Combined with Rigorously Controlled Crevice Geometry for Study of Crevice Corrosion Scaling Law¹⁵

Historically, one of the major challenges in crevice corrosion research has been the disconnect between the crevice geometries that can be modeled and those that can be attained experimentally. This situation led to a sharp disagreement about how the crevice gap controls the position of maximum attack within the crevice, even for simple electrochemical systems in which the experiment is arranged to prevent any solution composition change within the crevice.¹⁶ The relation between the position of maximum attack (x_{crit}) and the crevice gap (G) is known as the scaling law. Two distinct scaling laws for crevice corrosion had been suggested, x_{crit}^2/G^{16} ,¹⁷ and x_{crit}/G .¹⁶

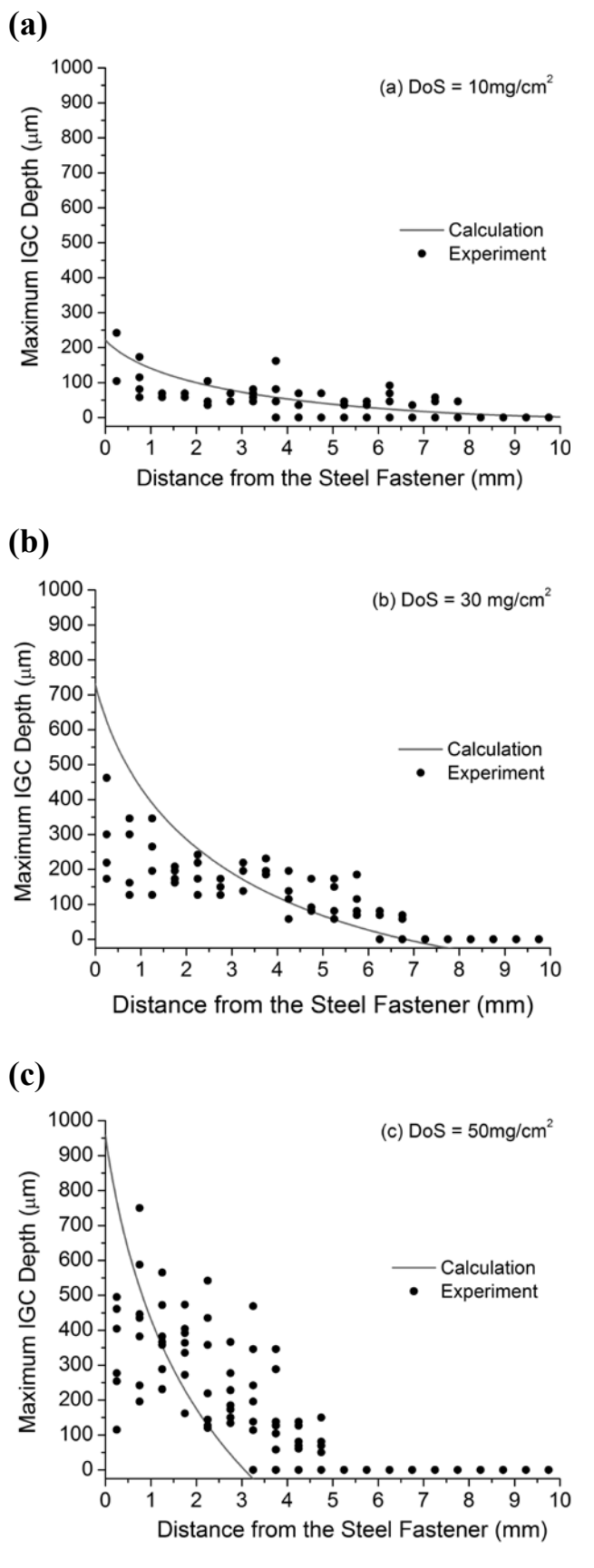


Fig. 2. Comparison of the IGC damage derived from the calculated potential distributions and the experimentally determined IGC damage after 100 h: (a) DoS = 10 mg/cm²; (b) DoS = 30 mg/cm²; (c) DoS = 50 mg/cm². In all cases, the LD was 3.5 DoS = 3.5 g/m².¹⁰

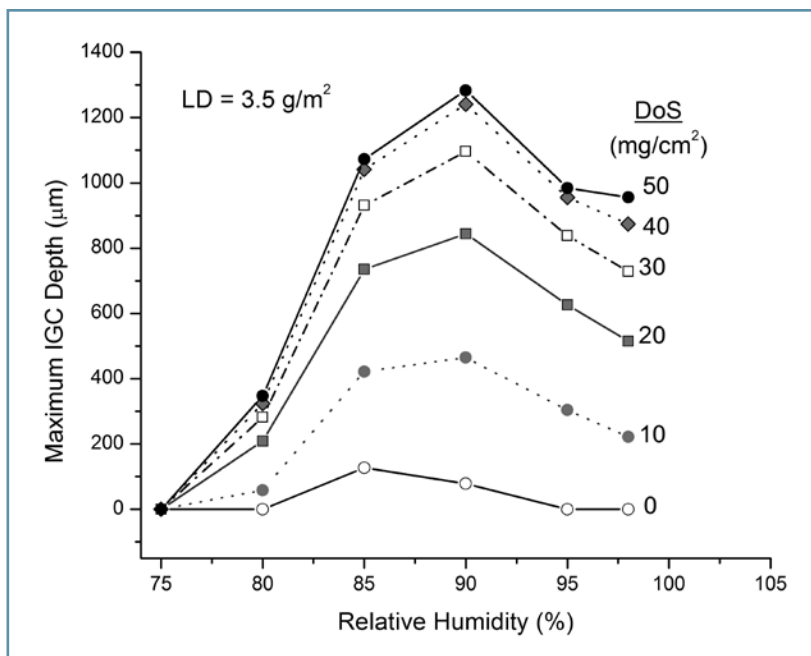


FIG. 3. Model calculation results for maximum IGC propagation after 100 h exposure as a function of RH (DoS = 0 to 50 mg/cm², LD = 3.5g/m²).¹⁰

The objective of the work in this example was to unambiguously assess which scaling law applies, particularly to small crevices. Lee, Reed, and Kelly¹⁵ combined FEM modeling and microfabrication methods to rigorously link computational results with experimental measurements. Microfabrication methods were used to construct crevice formers of rigorously controlled dimensions. These formers were used in crevice corrosion experiments on Ni200 in 0.5 M H₂SO₄ to measure x_{crit} for crevice gaps of 14, 35, 93, 153, and 395 µm. Comparison of the modeling and experimental results provided a better understanding of the geometric scaling factors that apply to crevice corrosion.

The FEM program used in this work was capable of considering two spatial dimensions and time,^{17,18} as in the earlier example, convection was ignored, and the potential and current distributions were calculated at $t = 0$, effectively reducing the governing equation to the Laplace equation. The geometry used is shown in Fig. 4. The fit to the potentiodynamic scan of Ni200 in sulfuric acid (which contains an active/passive transition) served as the electrochemical boundary condition for the model.

The potential and current density distributions obtained from the FEM model are shown in Fig. 5. The potential fell monotonically with increasing distance into the crevice, and the corresponding dissolution current density mapped out the passive-to-active transition. The x_{crit} value for each gap was determined by locating the position at which the potential fell into the active region bounded at +0.244 V (vs. SCE).

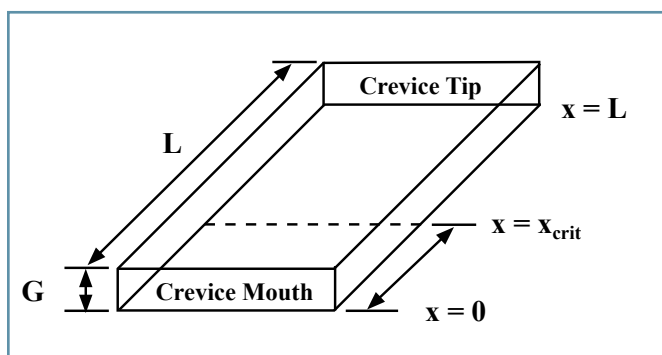


FIG. 4. Schematic diagram illustrating the important parameters of crevice corrosion scaling laws.¹⁵

A comparison of x_{crit} data from the crevice corrosion experiments and those predicted by the model is shown in Fig. 6a. Figure 6b plots the same data, but with the ordinate now in terms of x_{crit}^2 . At small gaps (< 100 µm) the data fit to a linear regression has a correlation coefficient of 0.9957 with the y intercept forced through zero. From these comparisons, it was concluded that a quadratic scaling factor ($x_{crit}^2/G = \text{constant}$) was applicable to the Ni/H₂SO₄ crevice system, with the result most apparent at short times and small gaps. The model also reproduced the experimentally observed failure of the scaling law at large gaps where the x_{crit} was located at much greater depths than would be expected from the scaling law. The potential and current distributions explain this observation. At the 153 µm gap crevice, the entire active/passive transition was not completed before the end of the crevice was reached, thus reducing the total current from the crevice and the subsequent potential drop.

State-of-Art Issues in Localized Corrosion Modeling

Application of numerical methods, especially FEM, has greatly facilitated understanding phenomena and mechanisms across a diverse spectrum of localized corrosion problems. However, important issues still remain in localized corrosion modeling that hinder comparisons of modeling results and experimental data. Most of the issues are rooted in assumptions and simplifications that are made in order to make the calculations more tractable.

One important issue comes from ignoring ion-ion interactions in the electrolyte. Generally, modeling of the ion transport process is based on the assumption of dilute solution conditions, and the Nernst-Planck equation is used as discussed to describe ion transport due to diffusion, migration, and convection. For the migration term, the flow of each ion due to electric potential field in the system is assumed to be independent. However, the electric potential field is also affected by distribution of all the ions as described by Poisson's equation which accounts for the relationship between charge densities and the electric potential

$$\nabla^2 \Phi = -\frac{F}{\epsilon} \sum_{i=1}^n z_i c_i \quad (4)$$

The rigorous approach to model transport phenomena in dilute solution environment is to solve the Nernst-Planck equation coupled with the Poisson's equation. However, attempts to obtain numerical solutions by applying these two equations have encountered substantial numerical stiffness¹⁹ when performing calculations. Thus, the more widely used approach invokes electroneutrality, which ignores electrostatic interaction between ions, as a replacement for Poisson's equation to describe ion transport in the electrochemical system. However, this coupling of the Nernst-Planck equation with an electroneutrality assumption loses sight of the fundamental physics. The basic form of the Nernst-Planck equation shown in Eq. 1 ignores ion-ion interactions. In practice, to use the Nernst-Planck equation in combination with the electroneutrality condition, at each time step for each spatial element, a "make-up" ion is selected to enforce electroneutrality. There is concern that this lacks a defensible physical basis, particularly when it is not obvious which ion should be selected. In some cases, negative concentrations can be predicted.

Several approaches have been proposed to take into account ion-ion interactions during ion transport in dilute solutions. Heppner and Evitts²¹ developed a charge density correction method based on Poisson's equation to calculate the effect of charge density on electrolyte mass transport. By using an operator splitting method,^{22,23} the value of a charge density correction can be determined to offset the charge of the electrolyte solution. Sarkar and Aquino²⁰ developed

(continued on next page)

a novel finite element approach to describe the mass transport process in dilute solutions with the consideration of ion-ion interactions. They incorporated Onsager's approach^{24,25} in which the total flux of an ion is a linear combination of all the thermodynamics driving forces, but assumed that the ion distributions in the electrochemical system are independent, neglecting the cross-coefficients in Onsager's formulation.²⁰ In their approach, a new thermodynamic parameter was defined, which can be interpreted as the rate of accumulation of one ion species at a local point in the domain due to ionic interactions. This parameter was then included in the Nernst-Planck equation, creating a modified mass transport equation. By solving the system of modified mass transport equations for all involved ion species, the electroneutrality condition, and Poisson's equation at the same time, the concentration and potential distribution profiles were calculated. Later, Sarkar and Aquino²⁶ applied this approach²⁰ to simulate the movement of a pit surface, as well as the time-dependent profiles of concentration, current, and potential distribution inside the pit.

Concluding Comments

FEM analyses have contributed a great deal to our understanding of localized corrosion conditions, including identification of key parameters. The availability of commercial FEM codes with electrochemical modules allow non-experts to input geometries, boundary conditions, and initial conditions. This development will no doubt increase the use of FEM for these studies. Further fundamental work is still needed, though, to address the effects of often implicit assumptions.

Acknowledgments

We wish to thank the Office of Naval Research (ONR) for its financial support through Grant N00014-14-1-0012. William Nikerson, Technical Office, is gratefully appreciated.

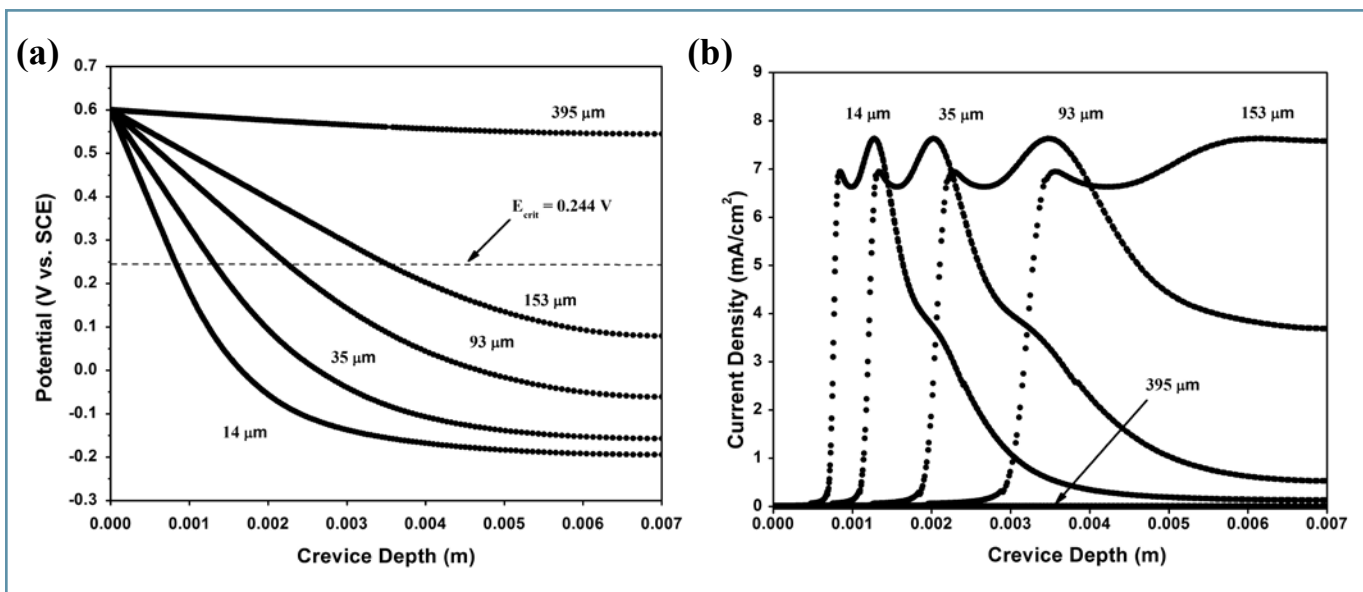


FIG. 5. (a) Potential distributions estimated by the model for gaps ranging from 14 to 395 μm . (b) Corresponding current density distributions for each gap.¹⁵

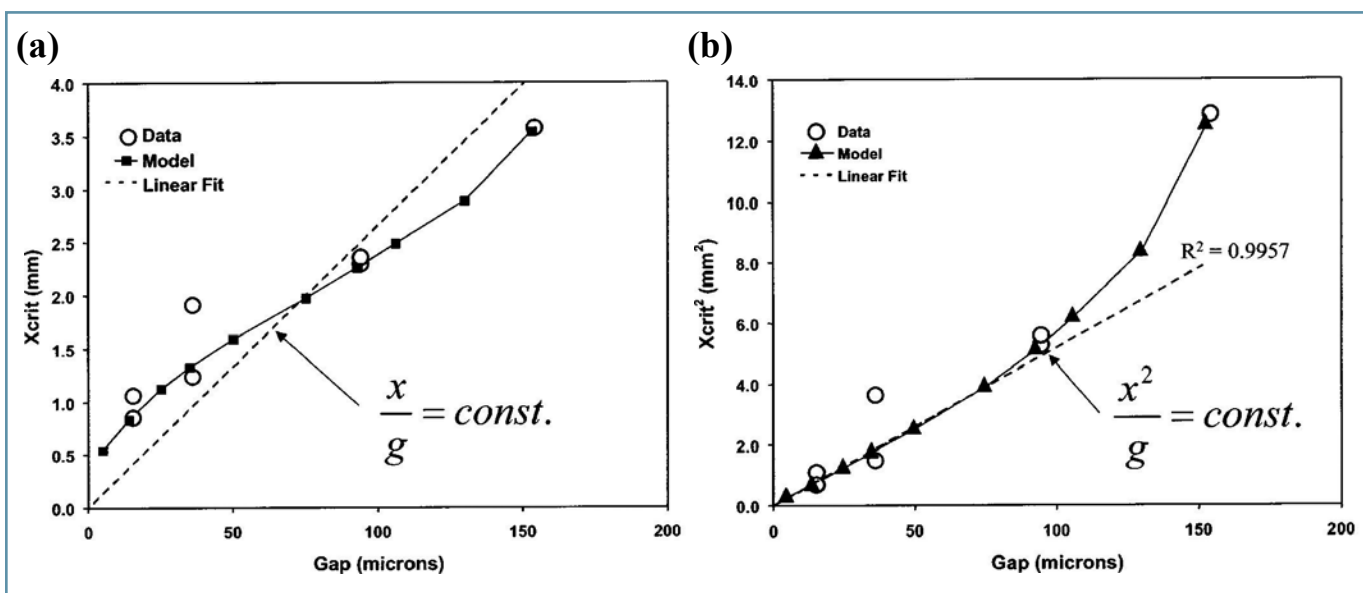


FIG. 6. (a) Comparison of experimental and computational data for x_{crit} for Ni200 in 0.5 M H_2SO_4 as a function of gap plotted on linear scales for both x_{crit} and gap. (b) Comparison of experimental and computational data of x_{crit} for Ni200 in 0.5 M H_2SO_4 as a function of gap plotted on a quadratic scale for x_{crit} and a linear scale for gap.¹⁵

About the Authors



CHAO LIU is a graduate research assistant supervised by R. G. Kelly in the Department of Materials Science and Engineering at the University of Virginia. His research mainly focuses on mathematical modeling of localized corrosion under atmospheric conditions. He serves on the executive board of the ECS student chapter at the University of Virginia and is also a student member of NACE International. He obtained his Bachelor's degree in applied chemistry from Nanchang University, China, and completed his Master's study in chemical engineering under M. E. Orazem at the University of Florida. He can be reached at cl5bc@virginia.edu.



R. G. KELLY is the AT&T Professor of Engineering in the Department of Materials Science and Engineering at the University of Virginia, whose faculty he joined in 1990. His present work includes studies of the electrochemical and chemical conditions inside localized corrosion sites, atmospheric corrosion, improved accelerated testing, and multi-scale modeling of corrosion processes. He is the Co-Director of the Center for Electrochemical Science and Engineering at UVa. He is a Fellow of ECS as well as NACE International. He completed his PhD studies at the Johns Hopkins University under Patrick Moran, Eliezer Gileadi, and Jerome Kruger. He then spent two years at the Corrosion and Protection Centre at the University of Manchester (UK) as a Fulbright Scholar and as an NSF/NATO Post-doctoral Fellow working with Roger Newman. He can be reached at rgkelly@virginia.edu.

References

1. D. A. Jones, *Principles and Prevention of Corrosion*, 2nd ed., Prentice-Hall, Inc., Upper Saddle River, NJ (1996).
2. M. L. C. Lim, J. R. Scully, and R. G. Kelly, *Corrosion*, **1**, 35 (2013).
3. R. Alkire, T. Bergh, and R. L. Sani, *J. Electrochem. Soc.*, **125**, 1981 (1978).
4. A. W. Forrest Jr., J. W. Fu, and R. T. Biccichi, Paper 150 presented at the NACE National Conference, Chicago, March, 1980.
5. J. W. Fu, Paper 115 presented at the NACE National Conference, Toronto, April, 1981.
6. J. Newman, and K. E. Thomas-Alyea, *Electrochemical Systems*, 3rd ed., Wiley-Interscience, Hoboken, N. J (2004).
7. J. N. Harb, and R. C. Alkire, *J. Electrochem. Soc.*, **138**, 3568 (1991).
8. F. Cui, F. J. Presuel-Moreno, and R. G. Kelly, *Corrosion*, **62**, 251 (2006).
9. F. J. Presuel-Moreno, H. Wang, M. A. Jakab, R. G. Kelly, and J. R. Scully, *J. Electrochem. Soc.*, **153**, B486 (2006).
10. D. Mizuno, and R. G. Kelly, *Corrosion*, **69**, 681 (2013).
11. M. Verbrugge, *Corros. Sci.*, **48**, 3489 (2006).
12. G. L. Song, *Adv. Eng. Mater.*, **7**, 563 (2005).
13. D. Mizuno, and R. G. Kelly, *Corrosion*, **69**, 580 (2013).
14. Z. Y. Chen, F. Cui, and R. G. Kelly, *J. Electrochem. Soc.*, **155**, C360 (2008).
15. J. S. Lee, M. L. Reed, and R. G. Kelly, *J. Electrochem. Soc.*, **151**, B423 (2004).
16. Y. Xu, and H. W. Pickering, *J. Electrochem. Soc.*, **140**, 658 (1993).
17. L. A. DeJong, M. S. Thesis, Department of Materials Science and Engineering, University of Virginia, Charlottesville, VA (1999).
18. K. C. Stewart, Ph.D. Dissertation, Department of Materials Science and Engineering, University of Virginia, Charlottesville, VA (1999).
19. S. W. Feldberg, *Electrochem. Commun.*, **2**, 453 (2000).
20. S. Sarkar, and W. Aquino, *Electrochim. Acta*, **56**, 8969 (2011).
21. K. L. Heppner, and R. W. Evitts, *Corros. Eng., Sci. Technol.*, **41**, 110 (2006).
22. R. W. Evitts, Ph.D. Dissertation, University of Saskatchewan, Saskatoon, Saskatchewan, Canada, (1997).
23. M. K. Watson, Ph.D. Dissertation, University of Saskatchewan, Saskatoon, Saskatchewan, Canada, (1989).
24. L. Onsager, *Phys. Rev.*, **37**, 405 (1931).
25. L. Onsager, and R. M. Fuoss, *J. Phys. Chem.*, **36**, 2689 (1932).
26. S. Sarkar, J. E. Warner, and W. Aquino, *Corros. Sci.*, **65**, 502 (2012).